Hindawi
Journal of Chemistry
Volume 2022, Article ID 8995440, 8 pages
https://doi.org/10.1155/2022/8995440

*Research Article*

# An Ultrafast Fluorescent Probe for the Detection of Peroxynitrite in Living Cells

**Xiaofeng Wang**,[1] **Shu Xiao**,[2] **Xuejun Zhou**,[1] **and Tingting Duan**[1]

[1]*Department of Otolaryngology-Head and Neck Surgery, The First Affiliated Hospital of Hainan Medical University, Haikou 570102, China*
[2]*Obstetrics Department of Hainan Modern Women and Children's Hospital, Haikou 570102, China*

Correspondence should be addressed to Xuejun Zhou; xuejunzhou@hainmc.edu.cn and Tingting Duan; denieceduan@163.com

Received 21 July 2022; Revised 23 September 2022; Accepted 22 October 2022; Published 16 November 2022

Academic Editor: José M. G. Martinho



Peroxynitrite ($ONOO^-$), a highly reactive nitrogen species, which plays a crucial role in numerous physiological and pathological processes of cell functionalization. The anomalous concentration of $ONOO^-$ may result in a range of diseases, such as arthritis, neurological disorders, and even cancer. Therefore, it is urgent to develop a simple and effective tool to monitor the fluctuation of $ONOO^-$ levels in biological systems. Herein, an ultrafast fluorescent probe (HND-ONOO) is proposed to detect $ONOO^-$, which displays brilliant fluorescence in less than 30 s with a large Stokes shift. Furthermore, the probe exhibited the lower detection limit (48 nM) and satisfactory results in differentiating $ONOO^-$ from other related species. The probe that possesses good biocompatibility and low toxicity was employed to monitor the level of exogenous and endogenous $ONOO^-$ in living cells. Thus, the probe HND-ONOO could be served as a potential imaging tool to visualize intracellular $ONOO^-$ and understand the relationship between $ONOO^-$ and inflammation.

## 1. Introduction

Reactive nitrogen species (RNS), extremely significant intracellular signaling molecules, are irreplaceable in various physiological and pathological processes, such as cell growth, differentiation, and apoptosis [1, 2]. However, external stimuli may cause abnormal levels, leading to a range of diseases, including arthritis, high blood pressure, and neurological diseases [3–5]. Peroxynitrite ($ONOO^-$), a common type of RNS, is generated from superoxide anion ($O_2^-$) and nitric oxide (NO) by intracellular diffusion [6–8]. As a strong oxidative and nitrative reagent, $ONOO^-$ can react with biological macromolecules such as proteins and DNA and is thought to be involved in signal transduction. [9,10] However, elevated levels of $ONOO^-$ may affect the normal activities of cells and organ aging, which in turn may lead to inflammatory diseases, autoimmune diseases, and cancer. [11–13] For example, rheumatoid arthritis served a general chronic inflammatory disease that may induce joint swelling, pain, and damage, bringing a lot of inconvenience to human life. [14, 15] Therefore, the development of a simple and effective tool to detect $ONOO^-$ in real-time in biological systems to understand its role in related diseases is urgently needed to understand the progress of the disease.

Over the decades, various analysis techniques have been employed to sense $ONOO^-$, such as UV-vis spectroscopy, electrochemical analysis, and electron spin resonance. [16–20] However, although these methods can be used for the detection of $ONOO^-$, they still have certain deficiencies due to the short half-life and low content of $ONOO^-$ in biological systems. In order to further understand the regulation mechanism of $ONOO^-$ in vivo, it is urgent to develop effective techniques to realize the rapid and precise detection of $ONOO^-$ in cells. The fluorescence probe and imaging method have attracted wide attention because of its noninvasiveness, excellent sensitivity and significant spatiotemporal resolution, and real-time visual inspection. [7, 21–25] So far, more and more fluorescent probe is

constructed for the detection of $ONOO^-$. [26–28] These reported probes are mainly based on $ONOO^-$ reaction with specific groups, including the cleavage of C=C, trifluoromethyl ketone, $\alpha$-ketoamide, and the oxidation of hydrazides, N-dearylation and boronate. [29–36] However, although some probes are proposed to sense trace amounts of $ONOO^-$, they are disturbed by other substances, such as hydrogen peroxide ($H_2O_2$) or hypochlorous acid (HClOH). [37–39] Furthermore, slow reaction speed, poor water solubility, and low biocompatibility limit the application of probes in biological systems. Therefore, there are still some challenges in developing fluorescent probes with good biocompatibility to achieve the rapid monitoring of $ONOO^-$ in living cells.

In this work, we propose a reasonable fluorescent probe (HND-ONOO) for rapid monitoring of intracellular $ONOO^-$. The probe consists of hemicyanine dye and a phenylboronic acid ester derivative as a specific response group for $ONOO^-$. Notably, this probe displays high selectivity and specificity for $ONOO^-$, especially when not disturbed by active species such as $H_2O_2$ and HClO. In addition, the probe cleaved the boronic ester group within 30 s, releasing the naked hydroxyl group and causing the turn-on of the fluorescent signal. HND-ONOO also exhibits a great linear relationship and lower detection limit (LOD) toward $ONOO^-$. Furthermore, the probe HND-ONOO was successfully utilized to monitor and image exogenous and endogenous of $ONOO^-$ in cells. We believe that this probe has great potential for discussing the relationship between $ONOO^-$ and inflammatory diseases and is helpful for the diagnosis of inflammation.

## 2. Experimental Section

*2.1. Apparatus and Reagents.* The UV-vis and fluorescence spectra were carried out on the UV-2910 and F-7000 fluorescence spectrophotometers, respectively. $^1$H NMR (500 MHz) and $^{13}$C NMR (125 MHz) were implemented on a Bruker nuclear magnetic resonance spectrometer. The fluorescence images of living were performed on an Olympus FV1000. The chemical reagents come from Maclean, and the main biological reagents come from Biyuntian.

*2.2. Synthesis of Compound 2.* We added 4.5 mL of iodoethane and 2.2 g of 2,3,3-trimethyl-3H-indole into a 100 mL round bottom flask, and then, 30 mL of acetonitrile was added to the mix. After refluxing for 12 h, a large amount of pink solids were generated. The solid obtained by filtration is used directly in the next step without further purification.

*2.3. Synthesis of HND.* The compound 2 (0.63 g) and 2-Hydroxy-6-naphthaldehyde (0.38 g) were put in a round bottom flask. Then, 8 mL of absolute ethanol was added to the mixture, and further heated to reflux for 9 h. The mixture was cooled to room temperature, and then, placed in ice water to cool; a lot of dark red solid was obtained. Subsequently, the solid was filtered by suction and washed with ice absolute ethanol to obtain compound HND. $^1$H NMR (500 MHz, DMSO-$d_6$) $\delta$ 9.56 (s, 1H), 7.93–7.80 (m, 2H), 7.61–7.50 (m, 2H), 7.43 (d, $J$ = 8.9 Hz, 1H), 7.37–7.35 (m, 1H), 7.12–7.06 (m, 1H), 6.99–6.92 (m, 2H), 6.86 (s, 1H), 6.40–6.33 (m, 2H), 4.26–4.02 (m, 2H), 1.64 (s, 3H), and 1.21 (s, 6H).

*2.4. Synthesis of HND-ONOO.* To a 50 mL round bottom flask was added 220 mg of compound 2 (0.66 mmol), 300 mg of 4-bromomethyl-phenylboronic acid pinacol ester (1 mmol), 276 mg of anhydrous $K_2CO_3$ (2 mmol), and 20 ml of acetonitrile. The mixture was heated to 80°C and refluxed overnight. The reaction was stopped, it was cooled to room temperature, and the solvent was removed under reduced pressure to obtain the crude product. The obtained crude product was purified by silica gel column chromatography ($CH_2Cl_2$ : $CH_3OH$ = 20:1, v/v) to obtain 150 mg of a solid compound (yield: 41%). $^1$H NMR (500 MHz, $CDCl_3$) $\delta$ 8.92 (s, 1H), 8.36–8.30 (t, $J$ = 14.8 Hz, 3H), 8.15–8.14 (d, $J$ = 8.9 Hz, 1H), 7.89–7.88 (d, $J$ = 7.9 Hz, 3H), 7.64–7.58 (t, $J$ = 14.6 Hz, 4H), 7.52–7.51 (d, $J$ = 7.9 Hz, 2H), 7.32–7.32 (d, $J$ = 2.2 Hz, 1H), 7.23–7.23 (d, $J$ = 2.2 Hz, 1H), 5.27 (s, 4H), 1.89 (s, 3H), 1.60 (s, 6H), 1.38 (s, 12H). $^{13}$C NMR (125 MHz, $CDCl_3$) $\delta$ 156.04 (s), 143.32 (s), 139.29 (s), 135.17 (s), 132.30 (s), 129.73 (s), 129.55 (d, $J$ = 8.9 Hz), 128.87 (s), 128.41 (s), 126.91 (s), 126.69 (s), 122.63 (s), 120.37 (s), 114.57 (s), 112.05 (s), 83.89 (s), 70.19 (s), 52.10 (s), 44.17 (s), 27.29 (s), 24.88 (s), and 14.48 (*s*). HRMS: m/*z* $C_{37}H_{41}BNO_3$ calcd, 558.3180; found $[M]^+$, 558.3181.

*2.5. Cell Culture and Confocal Imaging.* The HeLa and RAW 264.7 cells were incubated in DMEM containing with 10% FBS and 1% antibiotics (streptomycin/penicillin). The tested cells were placed at 37°C in a 95% humidified atmosphere with 5% $CO_2$. The cytotoxicity of HND-ONOO was assessed by the CCK-8 experiment. Those cells were put in a 96-well plate (10000 cells/well) for about 24 h. Subsequently, various levels of probe were added and then incubated for 24 h. After washing with DMEM medium, 10 $\mu$L CCK-8 was added to the cells. After incubating for about 4 h, the optical density was measured at 450 nm via a microplate reader (Tecan, Austria). The fluorescent image was carried out on the Olympus FV1000. The cells seeded in the culture dish and incubated for 24 h. Then, the cells stained by the probe were imaged after being washed with PBS for three times. Fluorescence collection window is 560-640 nm.

## 3. Results and Discussion

*3.1. Design and Synthesis of HND-ONOO.* The structure and the proposed response mechanism of probe HND-ONOO for $ONOO^-$ are shown in Scheme 1. In order to construct a sensitive and special fluorescent probe for $ONOO^-$, hemicyanine dye was chosen as the fluorophore due to its large Stokes shift, long emission properties, and great biocompatibility. Recent studies indicated that benzeneboronic acid and its ester are able to more quickly and efficiently respond to $ONOO^-$; therefore, it can serve as good candidate reaction

site for the sensitive and fast detection of $ONOO^-$. [40–42] 4-(bromomethyl) benzene-boronic acid pinacol ester was introduced as response group of $ONOO^-$ and the hemicyanine dye act as the light-emitting group. The probe HND-ONOO was nonfluorescent because of the 4-(bromomethyl) benzeneboronic acid pinacol ester inhibited the intramolecular charge transfer (ICT) process. The presence of $ONOO^-$ can first convert the phenylboronic ester to phenol, and then, the phenol derivative undergoes 1,6-self-elimination to release the fluorophore HND. The detailed synthetic route and $^1H$ NMR (Figure S1), [13]C NMR (Figure S2), and HRMS (Figure S3) characterizations of the probe are depicted in Supplementary Materials.

*3.2. Spectral Properties of HND-ONOO toward $ONOO^-$.* The spectral characteristics of HND-ONOO were discreetly discussed in PBS-DMSO buffer solution (pH = 7.4, PBS/DMSO = 9 : 1, v/v). The probe HND-ONOO exhibited an absorption centered at 450 nm. After reacting with $ONOO^-$, this absorption peak was significantly increased (Figure 1(a)). Furthermore, this absorption peak reduced with increasing $ONOO^-$ concentrations (0–20 $\mu$M). Subsequently, the fluorescence signal of HND-ONOO to variable levels of $ONOO^-$ was assessed. In the initial state, the probe HND-ONOO exhibited negligible fluorescence at the excitation of 440 nm. However, this probe HND-ONOO displayed a significant fluorescence emission centered at 590 nm in the presence of $ONOO^-$. The fluorescence intensity of the probe HND-ONOO obviously improved with the level of $ONOO^-$ elevated (Figure 1(b)), which should be ascribed to the rapid and specific reaction of $ONOO^-$ and (bromomethyl) benzeneboronic acid pinacol ester, resulting in the release of fluorescent signal. It also demonstrated that the probe HND-ONOO was capable of detecting $ONOO^-$. Furthermore, there obtained a great linear relationship between the fluorescence intensity of HND-ONOO and $ONOO^-$ content ranging from 0 to 20 $\mu$M (Figure 1(c)). The regression equation was established as $F_{590\ nm} = 12.9843[ONOO^-] + 31.6068$ with a satisfying linear relationship ($R^2 = 0.9863$). The detection limit (LOD) was affirmed as 48 nM according to the standard method of $3\sigma/k$, which suggested that proposed probe HND-ONOO was sufficient to identify trace $ONOO^-$. In addition, this property of HND-ONOO provided a possibility for further detection of intracellular $ONOO^-$.

*3.3. Selectivity.* Significant selectivity is one of the excellently pivotal factors in evaluating the merits of fluorescent probes. We first evaluated active species with similar properties to $ONOO^-$. As shown in Figure 1(d), significant fluorescence intensity enhancement was observed in the presence of $ONOO^-$. It was delightful that only $H_2O_2$ caused the probe fluorescence intensity to fluctuate slightly, while other reactive species, such as $^tBuOO\bullet$, $\bullet OH$, $NO_2^-$, NO; $O_2\bullet^-$, HNO, and HClO, cannot significantly alter the signal of the probe HND-ONOO. Furthermore, we tested whether common anions or cations ($Na^+$, $K^+$, $Ca^{2+}$, $HCO_3^-$, $Br^-$, and $HS^-$) and amino acid (glutamic acid (Glu), tryptophane (Trp), serine (Ser), methionine (Met), aspartic acid (Asp), threonine (Thr), and lysine (Lys) would respond to the probe (Figure S4(b)). Although previous studies [43] have shown that the probe may be destroyed by high concentrations of HClO, higher concentrations are required. As shown in Figure S4(c), the results demonstrated that low concentrations of HClO had only negligible effects on the probe. As we expected, there was negative fluorescence was obtained, further declaring that the probe HND-ONOO owned brilliant selectivity and specificity for $ONOO^-$.

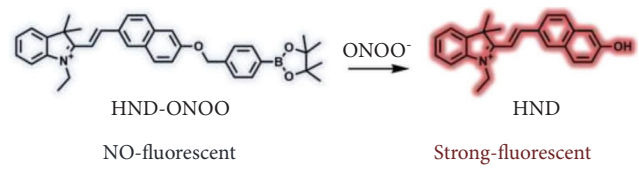


Scheme 1: The molecular structures of HND-ONOO and response mechanism to $ONOO^-$.

*3.4. The Response Speed and pH Effect.* The reaction kinetics of HND-ONOO to $ONOO^-$ was further accessed in PBS buffer (DMSO/PBS = 1 : 9, v/v, pH = 7.4). As shown in Figure 2(a), the fluorescence intensity was quickly improved and then achieved a plateau within 30 s, suggesting that HND-ONOO can fastly react with $ONOO^-$. Next, we added 20 $\mu$M $ONOO^-$ to verify, and similar experimental phenomena have been obtained. These results demonstrated the strong potential of the probe for real-time monitoring of $ONOO^-$ in cells. Subsequently, we investigated the effect of pH on HND-ONOO via fluorescence intensity fluctuations of HND-ONOO in the absence or presence of $ONOO^-$ ranging from 3.0 to 10.0. In the absence of $ONOO^-$, the fluorescence signal of HND-ONOO was weak and remained steady under the tested pH range. However, the fluorescence signal of HND-ONOO increases rapidly and remains constant under physiological pH (Figure 2(b)). The above result revealed that the probe HND-ONOO suitable for detecting trace amounts of $ONOO^-$ in physiological environments.

*3.5. Imaging of $ONOO^-$ in Living Cells.* Encouraged by the excellent spectral properties of HND-ONOO, the ability of the probe HND-ONOO to trace $ONOO^-$ in biological systems was further investigated. Initially, the Cell Counting Kit-8 (CCK-8) experiment was carried out to evaluate the cytotoxicity of the probe HND-ONOO. Herein, RAW 264.7 cells and HeLa cells were checked as study subjects. As shown in Figure S5, even when the concentration of the probe was as high as 50 $\mu$M, the cell viability was still more than 85%, which suggested the probe HND-ONOO had lower cytotoxicity. It can be applied to detect the content of $ONOO^-$ in living cells because of probe exhibits low cytotoxicity, high sensitivity, and specificity. Therefore, we further accessed the application of the probe for detecting $ONOO^-$ in HeLa cells and RAW 264.7 cells. Herein, the HeLa cells were pretreated with 3-morpholino-sydnonimine

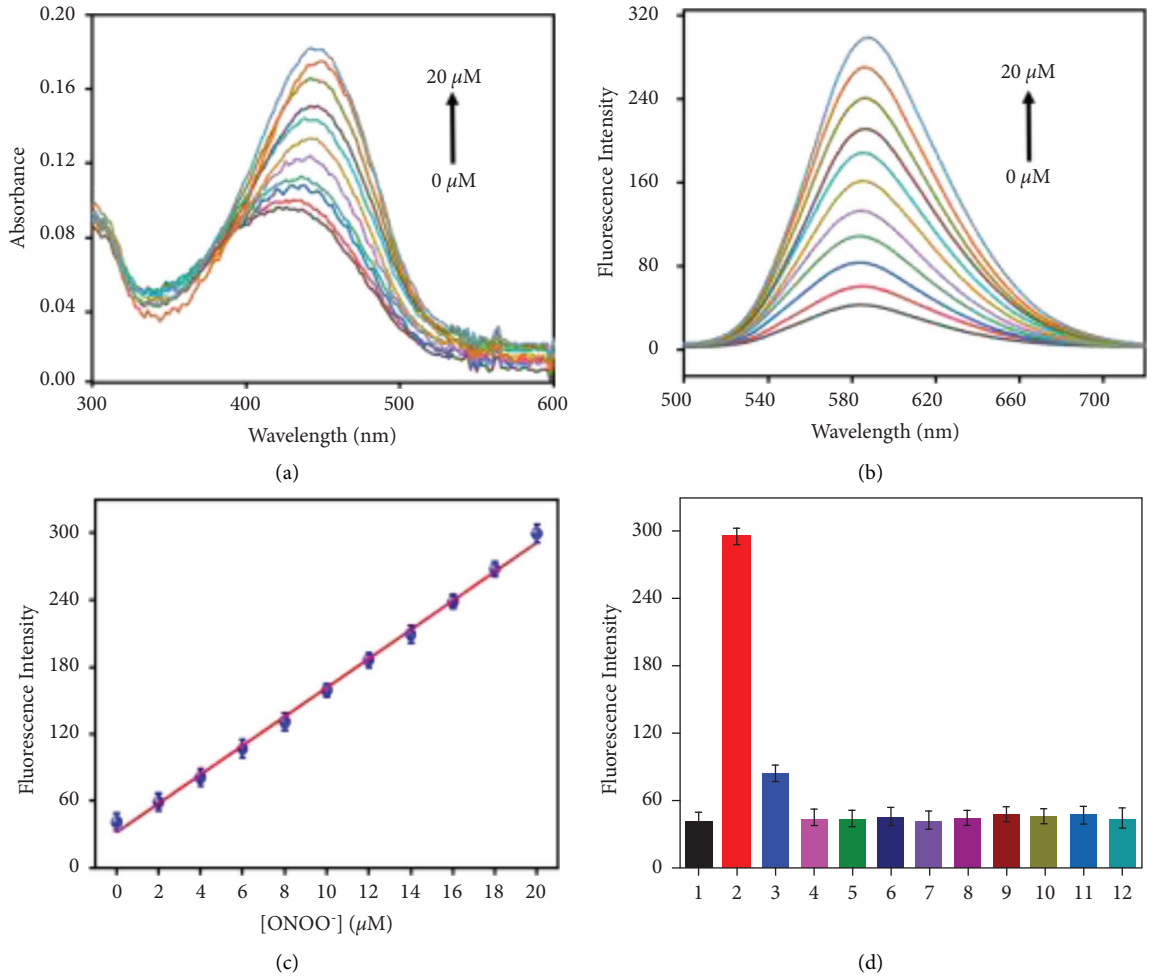


Figure 1: Spectral characteristics of HND-ONOO. (a) UV-Vis absorption and (b) the fluorescence spectrum of probe toward $ONOO^-$ (0–20 $\mu$M). (c) The linear relationship between the fluorescence intensity and $ONOO^-$. (d) The response of HND-ONOO to various active substance: 1, blank; 2, $ONOO^-$ (20 $\mu$M); 3, $H_2O_2$ (100 $\mu$M); 4, HClO (100 $\mu$M); 5, $O_2^{\bullet-}$ (100 $\mu$M); 6, •OH (100 $\mu$M); 7, $^tBuOO\bullet$ (100 $\mu$M); 8, NO (100 $\mu$M); 9, HNO (100 $\mu$M); 10, GSH (10 mM); 11, Hcy (10 mM); 12, Cys (10 mM).

(SIN-1, an $ONOO^-$ donor, 100 $\mu$M, 250 $\mu$M, and 500 $\mu$M) for about 30 min before imaging. A weak fluorescence signal was obtained for the control group that has not been processed. However, we observed the obvious fluorescence signal enhancement when these cells that were stained by the probe were treated with 100 $\mu$M SIN (Figure 3). Furthermore, to verify whether the fluorescence fluctuation with the change of $ONOO^-$ content, we added different concentrations of SIN to study the changes in the fluorescence signal. As we expected, the fluorescence intensity enhanced in existence 250 $\mu$M and 500 $\mu$M of SIN, which indicated that the probe can be employed to analyze fluctuations in intracellular $ONOO^-$ levels. This content has been added accordingly to the manuscript and Supplementary Materials.

Next, we investigated whether the probes responded to possible interferers in living cells. The RAW 264.7 cells were only treated with HND-ONOO, and the cells had no obvious changes in fluorescence signal. However, when the RAW 264.7 cells were pretreated with 3-morpholino-sydnonimine (SIN-1, an $ONOO^-$ donor) for around 30 min and then incubated with HND-ONOO (10 $\mu$M) before imaging, a significantly enhanced fluorescence signal was obtained (Figure 4). Subsequently, the cells were pretreated with $H_2O_2$, HClO, and NOC-18 (a NO donor) and then incubated with HND-ONOO before imaging, respectively. As expected, a weak fluorescence signal was found, once again proving that the change in the fluorescence signal of the probe was caused by $ONOO^-$ rather than other species. The abovementioned experiments showed that the probe could be used for the detection of exogenous $ONOO^-$ in cells.

Since the probe displayed the capability of detecting exogenous $ONOO^-$, it had the potential to image endogenous $ONOO^-$. The application of the probe HND-ONOO for monitoring endogenous $ONOO^-$ was further researched. The assay was performed in RAW 264.7 cells because of the cells could generate high levels of inducible nitric oxide synthase (iNOS) after being stimulated by lipopolysaccharide (LPS) and interferon-$\gamma$ (INF-$\gamma$) [44,45]. As the control group, the RAW 264.7 cell was pretreated with probe, and an inert fluorescent was observed (Figure 5(a)). However, a splendid fluorescence enhancement signal was found in RAW264.7 cells, after co-

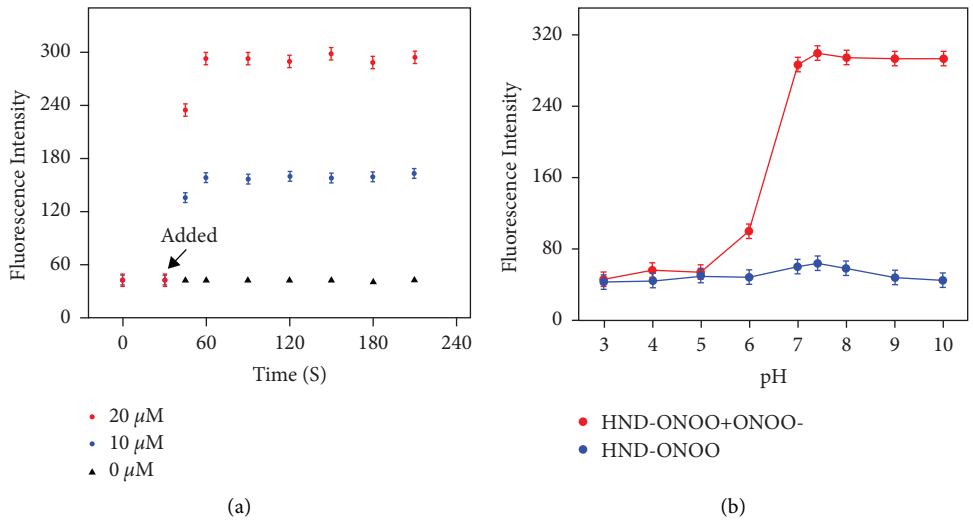


Figure 2: (a) The response speed and (b) pH effect of HND-ONOO to $ONOO^-$.

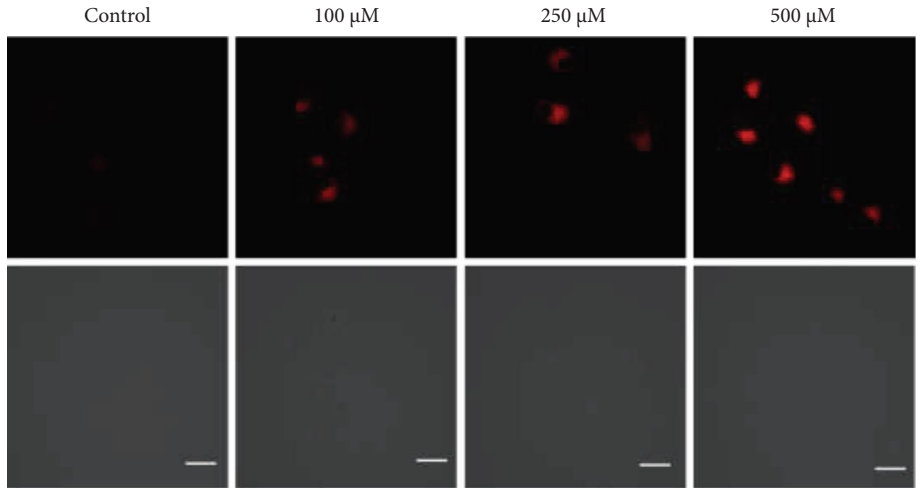


Figure 3: Imaging of exogenous $ONOO^-$ in HeLa cells. The cells were added with different level (100 $\mu$M, 250 $\mu$M, and 500 $\mu$M) of SIN. The scale bar is 20 $\mu$m.

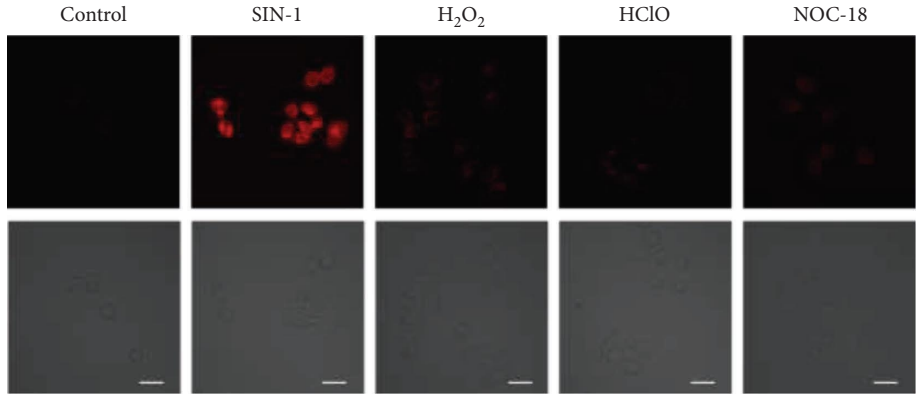


Figure 4: Fluorescent imaging of exogenous $ONOO^-$ in RAW 264.7 cells. The cells were treated with SIN-1, $H_2O_2$, HClO, NOC-18, and then, stained with HND-ONOO, respectively. The scale bar is 20 $\mu$m.

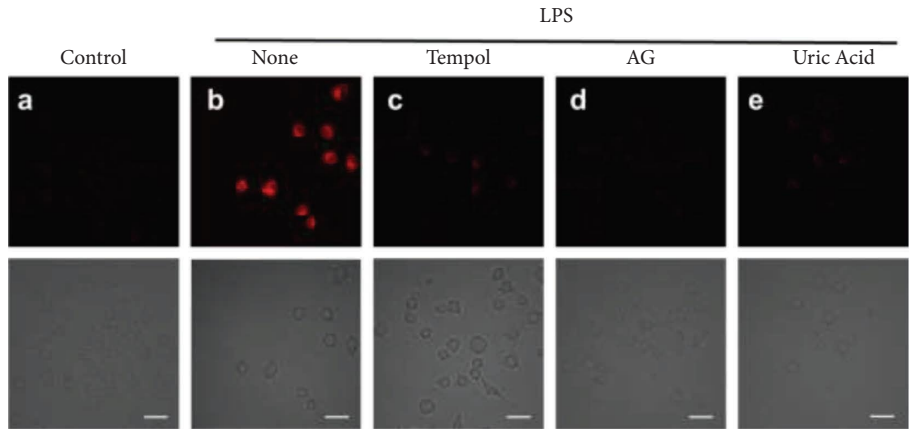


Figure 5: Imaging of endogenous $ONOO^-$ in RAW 264.7 cells. (a) Cells were preincubated with HND-ONOO. The cells were stimulated with LPS/INF-$\gamma$ and then incubated with HND-ONOO. The cells were stimulated with LPS/INF-$\gamma$ and treated with (c) Tempol, (d) AG, and (e) uric acid and then stained by HND-ONOO. The scale bar is 20 $\mu$m.

incubating with LPS/INF-$\gamma$, which suggested that the level of intracellular $ONOO^-$ was increased in the stimulation of oxidative stress (Figure 5(b)). Next, the RAW 264.7 cell line induced by LPS/INF-$\gamma$ was pretreated with aminoguanidine (a nitric oxide synthase (NOS) inhibitor AG, 0.5 mM), then treated with HND-ONOO. The falling fluorescence signal was found, which revealed that AG inhibited the generation of NOS and further reduced the level of $ONOO^-$ (Figure 5(d)). Similarly, the superoxide scavenger 2,2,6,6-tetramethylpiperidine-N-oxyl (Tempol) was used to verify whether its fluorescence signal was caused by $ONOO^-$ because the generation of $ONOO^-$ is inseparable from the participation of $O_2\bullet^-$ (Figure 5(c)). A weaker fluorescence experimental phenomenon was obtained, suggesting the levels of $ONOO^-$ was inhibited. Meanwhile, it also proved that intracellular fluorescence signal caused $ONOO^-$ rather instead of ROS. Finally, the intracellular fluorescence signal was obviously inhibited when an $ONOO^-$ scavenger (uric acid) was added (Figure 5(e)). All the above result evidenced that HND-ONOO can monitor fluctuations of endogenous and exogenous $ONOO^-$ in living cells.

## 4. Conclusions

In summary, we proposed a novel fluorescent probe HND-ONOO was employed to track intracellular $ONOO^-$ contents. The probe has excellent specificity and sensitivity and responds rapidly to $ONOO^-$ over various relevant analytes. The lower LOD and great linearity of the probe to $ONOO^-$ provide a certain basis for the analysis and detection of $ONOO^-$. Furthermore, its low biocompatibility cytotoxicity will benefit the monitoring of $ONOO^-$ under imaging studies and complex biological conditions. Furthermore, the proposed probe HND-ONOO was applied for imaging and detecting exogenous and upregulation of $ONOO^-$ via LPS stimulation in living cells. Therefore, these favorable properties of HND-ONOO to $ONOO^-$ make it promising for bioimaging research, in particular, to study its relationship with inflammatory diseases.

## Data Availability

The all data used to support the findings of this study are included within the article.

## Conflicts of Interest

The authors declare that they have no conflicts of interest.

## Authors' Contributions

Xiaofeng Wang and Shu Xiao contributed equally to this work.

## Acknowledgments

This work was supported by the Natural Science Foundation of Hainan Province (820MS141).

## Supplementary Materials

Structure characterizations of the probe, additional fluorescence spectra, and images. (*Supplementary Materials*)

## References

[1] Y. Hu, Y. Wang, X. Wen et al., *Research*, 2020, https://en.wikipedia.org/wiki/Research, Article ID 4087069.

[2] C. Hwang, A. J. Sinskey, and H. F. Lodish, "Oxidized redox state of glutathione in the endoplasmic reticulum," *Science (New York, N.Y.)*, vol. 257, no. 5076, pp. 1496–1502, 1992.

[3] A. Hausladen, A. J. Gow, and J. S. Stamler, "Nitrosative stress: metabolic pathway involving the flavohemoglobin," *Proceedings of the National Academy of Sciences*, vol. 95, no. 24, pp. 14100–14105, 1998.

[4] P. Pacher, J. S. Beckman, and L. Liaudet, "Nitric oxide and peroxynitrite in health and disease," *Physiological Reviews*, vol. 87, no. 1, pp. 315–424, 2007.

[5] X. Chen, F. Wang, J. Y. Hyun et al., "Recent progress in the development of fluorescent, luminescent and colorimetric probes for detection of reactive oxygen and nitrogen species," *Chemical Society Reviews*, vol. 45, no. 10, pp. 2976–3016, 2016.

[6] C. Szabó, H. Ischiropoulos, and R. Radi, "Peroxynitrite: biochemistry, pathophysiology and development of therapeutics," *Nature Reviews Drug Discovery*, vol. 6, no. 8, pp. 662–680, 2007.

[7] X. Luo, Z. Cheng, R. Wang, and F. Yu, "Indication of dynamic peroxynitrite fluctuations in the rat epilepsy model with a near-infrared two-photon fluorescent probe," *Analytical Chemistry*, vol. 93, no. 4, pp. 2490–2499, 2021.

[8] G. L. Squadrito and W. A. Pryor, "The formation of peroxynitrite in vivo from nitric oxide and superoxide," *Chemico-Biological Interactions*, vol. 96, no. 2, pp. 203–206, 1995.

[9] D. Gius and D. R. Spitz, "Redox signaling in cancer biology," *Antioxidants and Redox Signaling*, vol. 8, pp. 1249–1252, 2006.

[10] G. Ferrer-Sueta and R. Radi, "Chemical biology of peroxynitrite: kinetics, diffusion, and radicals," *ACS Chemical Biology*, vol. 4, no. 3, pp. 161–177, 2009.

[11] S. J. Klebanoff, "Myeloperoxidase: friend and foe," *Journal of Leukocyte Biology*, vol. 77, no. 5, pp. 598–625, 2005.

[12] T. Nagano, "Bioimaging probes for reactive oxygen species and reactive nitrogen species," *Journal of Clinical Biochemistry & Nutrition*, vol. 45, no. 2, pp. 111–124, 2009.

[13] D. Cheng, W. Xu, L. Yuan, and X. Zhang, "Investigation of drug-induced hepatotoxicity and its remediation pathway with reaction-based fluorescent probes," *Analytical Chemistry*, vol. 89, no. 14, pp. 7693–7700, 2017.

[14] J. S. Smolen, D. Aletaha, and I. B. McInnes, "Rheumatoid arthritis," *The Lancet*, vol. 388, no. 10055, pp. 2023–2038, 2016.

[15] Y. B. Joo and K. S. Park, "Gold thread acupuncture for rheumatoid arthritis," *New England Journal of Medicine*, vol. 377, no. 19, p. e27, 2017.

[16] L. Viera, Y. Z. Ye, A. G. Estévez, and J. S. Beckman, *Methods in Enzymology*, vol. 301, pp. 373–381, 1999.

[17] M. K. Hulvey, C. N. Frankenfeld, and S. M. Lunte, "Separation and detection of peroxynitrite using microchip electrophoresis with amperometric detection," *Analytical Chemistry*, vol. 82, no. 5, pp. 1608–1611, 2010.

[18] W. Imaram, C. Gersch, K. M. Kim, R. J. Johnson, G. N. Henderson, and A. Angerhofer, "Radicals in the reaction between peroxynitrite and uric acid identified by electron spin resonance spectroscopy and liquid chromatography mass spectrometry," *Free Radical Biology and Medicine*, vol. 49, no. 2, pp. 275–281, 2010.

[19] Y. R. Chen, C. L. Chen, W. Chen et al., "Formation of protein tyrosine ortho-semiquinone radical and nitrotyrosine from cytochrome c-derived tyrosyl radical," *Journal of Biological Chemistry*, vol. 279, no. 17, pp. 18054–18062, 2004.

[20] D. S. Bohle, B. Hansert, S. C. Paulson, and B. D. Smith, "Biomimetic synthesis of the putative cytotoxin peroxynitrite, ONOO-and its characterization as a tetramethylammonium salt," *Journal of the American Chemical Society*, vol. 116, no. 16, pp. 7423-7424, 1994.

[21] Y. Zhang, X. Zhang, H. Yang et al., "Advanced biotechnology-assisted precise sonodynamic therapy," *Chemical Society Reviews*, vol. 50, no. 20, pp. 11227–11248, 2021.

[22] J. Du, M. Hu, J. Fan, and X. Peng, "Fluorescent chemodosimeters using "mild" chemical events for the detection of small anions and cations in biological and environmental media," *Chemical Society Reviews*, vol. 41, no. 12, pp. 4511–4535, 2012.

[23] X. Chen, K. A. Lee, X. Ren et al., "Synthesis of a highly HOCl-selective fluorescent probe and its use for imaging HOCl in cells and organisms," *Nature Protocols*, vol. 11, no. 7, pp. 1219–1228, 2016.

[24] A. T. Aron, M. O. Loehr, J. Bogena, and C. J. Chang, "An endoperoxide reactivity-based FRET probe for ratiometric fluorescence imaging of labile iron pools in living cells," *Journal of the American Chemical Society*, vol. 138, no. 43, pp. 14338–14346, 2016.

[25] X. Song, S. Bai, N. He et al., "Real-time evaluation of hydrogen peroxide injuries in pulmonary fibrosis mice models with a mitochondria-targeted near-infrared fluorescent probe," *ACS Sensors*, vol. 6, no. 3, pp. 1228–1239, 2021.

[26] X. Xie, G. Liu, Y. Niu et al., "Dual-channel imaging of amyloid-$\beta$ plaques and peroxynitrite to illuminate their correlations in alzheimer's disease using a unimolecular two-photon fluorescent probe," *Analytical Chemistry*, vol. 93, no. 45, pp. 15088–15095, 2021.

[27] P. Wang, L. Yu, J. Gong et al., "An activity-based fluorescent probe for imaging fluctuations of peroxynitrite ($ONOO^-$) in the alzheimer's disease brain," *Angewandte Chemie*, vol. 61, no. 36, Article ID e202206894, 2022.

[28] X. Liu, L. He, X. Gong et al., "Engineering of reversible luminescent probes for real-time intravital imaging of liver injury and repair," *CCS Chemistry*, vol. 4, no. 1, pp. 356–368, 2022.

[29] D. Cheng, Y. Pan, L. Wang et al., "Selective visualization of the endogenous peroxynitrite in an inflamed mouse model by a mitochondria-targetable two-photon ratiometric fluorescent probe," *Journal of the American Chemical Society*, vol. 139, no. 1, pp. 285–292, 2017.

[30] B. Guo, J. Jing, L. Nie et al., "A lysosome targetable versatile fluorescent probe for imaging viscosity and peroxynitrite with different fluorescence signals in living cells," *Journal of Materials Chemistry B*, vol. 6, no. 4, pp. 580–585, 2018.

[31] Y. Li, X. Xie, X. Yang et al., "Two-photon fluorescent probe for revealing drug-induced hepatotoxicity via mapping fluctuation of peroxynitrite," *Chemical Science*, vol. 8, no. 5, pp. 4006–4011, 2017.

[32] D. Liu, S. Feng, and G. Feng, "A rapid responsive colorimetric and near-infrared fluorescent turn-on probe for imaging exogenous and endogenous peroxynitrite in living cells," *Sensors and Actuators B: Chemical*, vol. 269, pp. 15–21, 2018.

[33] T. Peng, X. Chen, L. Gao et al., "A rationally designed rhodamine-based fluorescent probe for molecular imaging of peroxynitrite in live cells and tissues," *Chemical Science*, vol. 7, no. 8, pp. 5407–5413, 2016.

[34] X. Han, Y. Ma, Y. Chen, X. Wang, and Z. Wang, "Enhancement of the aggregation-induced emission by hydrogen bond for visualizing hypochlorous acid in an inflammation model and a hepatocellular carcinoma model," *Analytical Chemistry*, vol. 92, no. 3, pp. 2830–2838, 2020.

[35] N. Zhao, Y. Li, W. Yin et al., "Controllable coumarin-based NIR fluorophores: selective subcellular imaging, cell membrane potential indication, and enhanced photodynamic therapy," *ACS Applied Materials & Interfaces*, vol. 12, no. 2, pp. 2076–2086, 2020.

[36] F. Yu, P. Li, B. Wang, and K. Han, "Reversible near-infrared fluorescent probe introducing tellurium to mimetic glutathione peroxidase for monitoring the redox cycles between peroxynitrite and glutathione in vivo," *Journal of the American Chemical Society*, vol. 135, no. 20, pp. 7674–7680, 2013.

[37] R. Yuan, Y. Ma, J. Du et al., "A novel highly selective near-infrared and naked-eye fluorescence probe for imaging peroxynitrite," *Analytical Methods*, vol. 11, no. 11, pp. 1522–1529, 2019.

[38] D. Wu, J. C. Ryu, Y. W. Chung et al., "A far-red-emitting fluorescence probe for sensitive and selective detection of

peroxynitrite in live cells and tissues," *Analytical Chemistry*, vol. 89, no. 20, pp. 10924–10931, 2017.

[39] X. Xie, X. Yang, T. Wu et al., "Rational design of an $\alpha$-ketoamide-based near-infrared fluorescent probe specific for hydrogen peroxide in living systems," *Analytical Chemistry*, vol. 88, no. 16, pp. 8019–8025, 2016.

[40] Z. Wang, F. Zhang, J. Xiong, Z. Mao, and Z. Liu, "Investigations of drug-induced liver injury by a peroxynitrite activatable two-photon fluorescence probe," *Spectrochimica Acta Part A: Molecular and Biomolecular Spectroscopy*, vol. 246, Article ID 118960, 2021.

[41] L. C. Murfin, M. Weber, S. J. Park et al., "Azulene-Derived fluorescent probe for bioimaging: detection of reactive oxygen and nitrogen species by two-photon microscopy," *Journal of the American Chemical Society*, vol. 141, no. 49, pp. 19389–19396, 2019.

[42] A. C. Sedgwick, X. Sun, G. Kim, J. Yoon, S. D. Bull, and T. D. James, "Boronate based fluorescence (ESIPT) probe for peroxynitrite," *Chemical Communications*, vol. 52, no. 83, pp. 12350–12352, 2016.

[43] H. R. Bolland, E. M. Hammond, and A. C. Sedgwick, "A fluorescent probe strategy for the detection and discrimination of hydrogen peroxide and peroxynitrite in cells," *Chemical Communications*, vol. 58, no. 76, pp. 10699–10702, 2022.

[44] R. B. Lorsbach, W. J. Murphy, C. J. Lowenstein, S. H. Snyder, and S. W. Russell, "Expression of the nitric oxide synthase gene in mouse macrophages activated for tumor cell killing. Molecular basis for the synergy between interferon-gamma and lipopolysaccharide," *Journal of Biological Chemistry*, vol. 268, no. 3, pp. 1908–1913, 1993.

[45] Y. Fu, H. Nie, R. Zhang et al., "An ESIPT based naphthalimide chemosensor for visualizing endogenous $ONOO^-$ in living cells," *RSC Advances*, vol. 8, no. 4, pp. 1826–1832, 2018.